AEROELASTIC ANALYSIS OF TWIN TURBOPROP UTILITY AIRCRAFT

Jiri Cecrdle, Jaromir Malecek, Otakar Cerny
Aeronautical Research and Test Institute
Beranovych 130, 199 05 Prague – Letnany, Czech Republic
e-mail: cecrdle@vzlu.cz, malecek@vzlu.cz, cerny@vzlu.cz

ABSTRACT

The submitted paper deals with aeroelastic certification analyses of a new generation Czech twin turboprop utility aircraft. Paper is focused to the calculations before the ground vibration test (GVT) of the prototype. It describes the analytical model and used tools and methods. The description of specific blocks of analyses follows afterwards. It includes preliminary flutter analyses, static aeroelastic analyses, modal analyses, flutter large parametric analyses. The flutter characteristics of the structure with respect to the selected parameters changes are presented. Besides the preparation of the GVT, the optimization of the exciters and accelerometers positions based on the analytical results and the whirl flutter analyses by means of optimization-based approach to find the critical stability boundaries are explained. Finally, the performed activities are summarized and the next phase of aeroelastic certification and the aircraft development are outlined.

1 INTRODUCTION

The presented aircraft, named EV-55 (see fig.1) is designed and manufactured by companies joined in the Association of Aviation Manufacturers of the Czech republic. It is designed as more reliable and powerful than existing same-class machines, low-priced and low operation costs transport aircraft. Different kind of operation like passenger, cargo or combi can be equally envisaged. With a total length of 14.35 m, the wingspan of 16.10 m and MTOW 4600 kg, it will travel with maximum speed of over 220 kts. The power unit consists of the turboprop engines P&WC PT6A-21 (536 shp each) and the four-blade constant speed propeller. It is a STOL aircraft able to operate from paved and unpaved runway types and is designed and certified according to CS/FAR 23 regulation. Fuselage is semi-monocoque metal structure with a share of composites. The wing is integral, trapezoidal-shaped, all-metal structure with the composite wing tips. In the wing between spars there are integral fuel tanks. The wing is equipped with split Fowler flaps and ailerons. Currently, project is staged at the point of completing the first airframe. The finalization of the first prototype is expected by the second half of 2009.

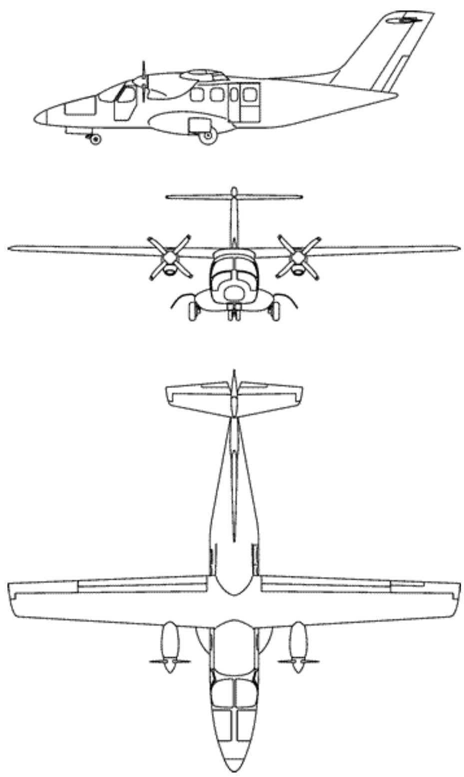

Fig.1: Aircraft outline

Aeroelastic analyses and the GVT are ensured by Aeronautical Research and Test Institute. Analyses are divided into the following main stages:

1) “Preliminary design” phase (2006 – 2007) – analytical model is based on a preliminary design; calculations are intended to avoid a possible aeroelastic problems as early as possible. The less critical aeroelastic phenomena (static – reversion, divergence) are analyzed as well.

2) “Pre-GVT” phase (2008 – 2009) – analytical model is based on the theoretical data of the final design. The main effort is paid to the parametrical flutter studies. Influence of the various structural

parameters is evaluated to specify the critical areas with respect to the flutter behavior.

3) "Post-GVT" phase (2010) – analytical model will be updated according the GVT results. The final calculations will be performed and results submitted to the certification authority.

2 ANALYTICAL MODEL

The analytical model is assigned for the FE analyses by means of the NASTRAN system. The structural model (see fig.2a) is a dynamic beam model. Stiffness is modeled via mass-less beams; inertia is modeled via concentrated mass elements. Control drives and engine attachments are modeled via spring elements. Model includes a various conditions (controls attachment, visualization elements, connection of structural parts etc.). Model is prepared as a half-model, with the half mass and stiffness parameters in the plane of symmetry and with the symmetric and antisymmetric boundary condition respectively. Various configurations regarding the fuel filling, longitudinal angle, payload, controls balancing, etc. are available.

Aerodynamic model (see fig.2b) is based on the Wing – Body Interference Theory. Lifting surfaces are modeled by means of the Doublett – Lattice panels, controls and tabs are modeled separately. Fuselage and nacelle are modeled as Slender and Interference bodies. Model includes the correction factors to account for the propeller slipstream. Interpolation between both models was realized by means of the beam splines.

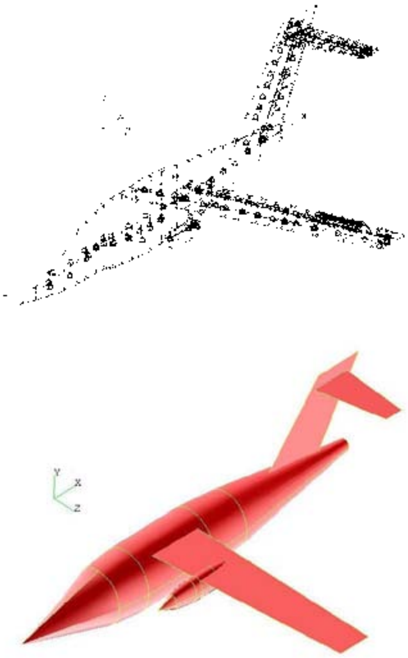

Fig.2: Structural and aerodynamic FE model (axonometry)

3 STATIC AEROELASTICITY

Static aeroelasticity calculations included the reversion of the controls and divergence of the lifting surfaces. Since the static aeroelastic phenomena are not so critical for the presented aircraft category, calculations were performed in the 1st phase using the preliminary model. The expected lower accuracy of the stiffness characteristics was taken into consideration by the configurations with reduced stiffness by 15 and 30% with respect to the nominal. The aileron, elevator and rudder reversion were calculated by means of the NASTRAN SOL 144. For the aileron reversion, the aileron surface was defined as deflected; the trim parameters were set to make the steady roll. Mach number was considered M=0 (incompressible flow) or M=0.4013 (compressibility correction, 1.2*V_D=150 m/s, flight altitude of H=0 m). The output parameter was the dimensionless roll rate (pb/2V). Increasing the dynamic pressure, the dimensionless roll rate makes decrease, the rate of zero defines the critical state of reversion. The similar approach was applied for other controls as well. It must be noted,

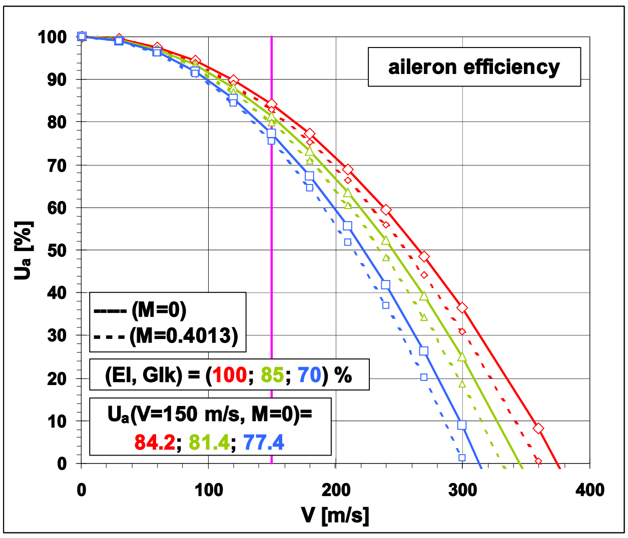

Fig.3: Aileron efficiency

that the results for velocities above the certification speed must be considered as artificial due to the subsonic aerodynamic theory usage. This note holds true for the flutter calculations as well. The efficiency of aileron is presented in the fig.3.

The divergence was calculated by means of the SOL 144 as well. The M, (EI,GI_k) and H parameters were considered the same as mentioned above. The results were the divergence dynamic pressures for the wing and vertical tail. It gives sufficient level of reserve towards the certification speed.

4 MODAL ANALYSIS

The normal modes analysis was performed by the SOL 103 (Lanczos method). Modes were calculated separately for the symmetric and antisymmetric boundary condition; in the frequency range up to 100 Hz. There were the wing tank loading and angle of climb, payload, wing-fuselage joint stiffness and overall structure stiffness taken under consideration as parameters, 16 mass configuration (symmetric and antisymmetric) in total.

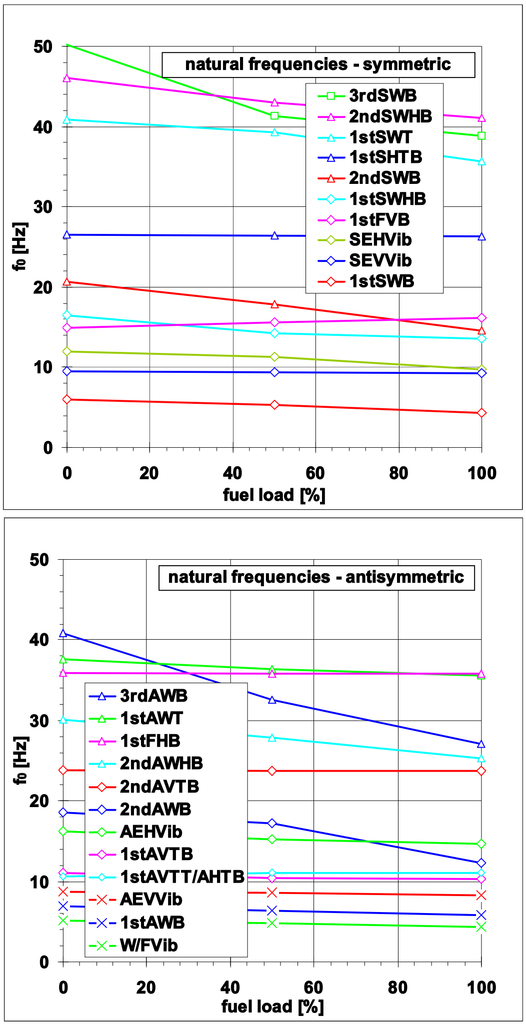

Fig.4: Modal characteristics – symmetric and antisymmetric

Results of these analyses were exploited for basic assessment of the dynamic characteristics of the structure, selection of main mass configurations for flutter analyses and flutter analyses planning, for the GVT planning, and also for calculation of the controls dynamic balancing. As an example, the natural frequencies of the main structural parts dependence on the wing fuel loading are listed in the fig.4 (frequency range up to 50 Hz only). Stiffness of the controls and tabs drives were estimated applying experiences from the previous aircraft taking into account the type of drive system (rods, ropes), length, control mass and size etc. These parameters will become a parameter for the flutter analyses until the reliable data will be at disposal (from tests etc.). For the mode shape visualization, the specific graphic format, generated by in-house postprocessing tool, was used (see fig.5). This format is useful for the direct visual comparison of mode shapes.

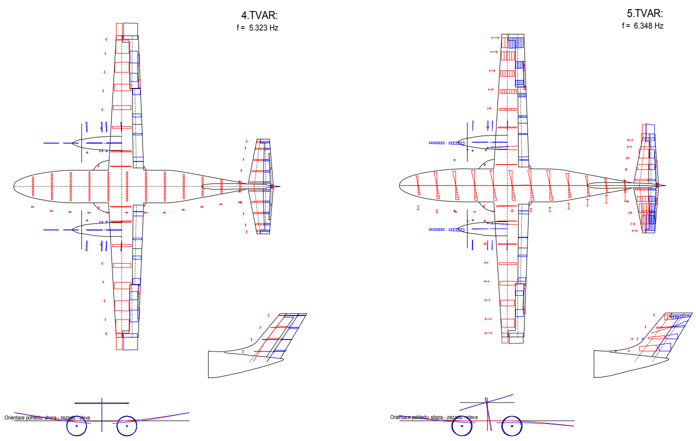

Fig.5: Mode shapes visualization – 1^{st}SWB; 1^{st}AVTB

5 CONTROLS DYNAMIC BALANCING

The calculations of the controls dynamic balancing towards the main mode shapes were performed. The node lines positions were obtained from the visualization like shown in the fig.5. Aileron is under-balanced towards torsional shapes, more critical are symmetric shapes due to the node line near the trailing edge in the wing tip part, regarding the fuel load, the worst mass configuration is fuel load of 100%. The elevator is slightly under-balanced towards the 1st FVB, rudder is under balanced towards the 1st FT. In comparison with aileron, these cases seem to be less critical either due to low level of under-balancing or the high difference in natural frequencies of studied modes.

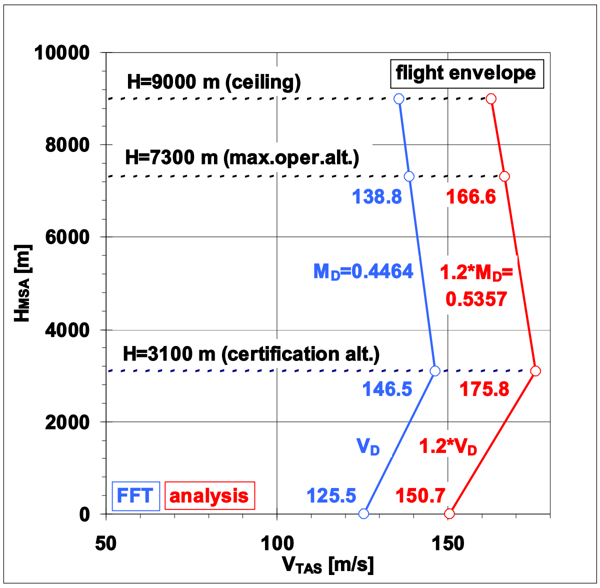

Fig.6: Flight envelope (V-H)

6 FLUTTER

The mass configurations for the flutter analyses were selected considering the calculations of mode shapes and the controls dynamic balancing. The flutter calculations were performed by the SOL 145 (PK method). The flight envelope for the flutter analysis according the CS 23 regulation is shown in the fig.6. Certification speed is restricted by the maximum speed or by the maximum Mach number. Large parametric calculations covering the changes and uncertainties of parameters (controls balancing, controls drive stiffness, mass and side configuration, flight altitude, etc.) were performed. At the practicable ranges of the parameters, there were found just the different types of the surface flutter, the level of reserve was sufficient. Parameters ranges were extended then to unrealistic values (large controls under-balancing) to find the occurrence areas of the control surfaces flutter and evaluate the level of reserve towards the controls balancing. The controls flutter was calculated for the 6 levels of the flight altitude. Structural damping was introduced by the viscous model, regarding the damping expected on the full-scale structure, it was estimated on the side of the safety with the damping ratio of 0.5%.

6.1 Surface flutter

First of all, it is effective to investigate the flutter of the basic structure. During these calculations, controls are aerodynamically blocked; it means that they vibrate as an integral part of the surface. There was investigated influence of the following parameters to the flutter behavior: The wing tank loading (0; 50; 100%) and angle of climb (-10; 0; +15 deg), payload (min.; max.), and overall structure stiffness (80; 100; 120% of nominal). Each parameters configuration had four variants (left / right side specification and symmetric / antisymmetric boundary condition), 198 calculations in total. Flutter was investigated in the velocity range up to 300 m/s and frequency up to 100 Hz. There were found

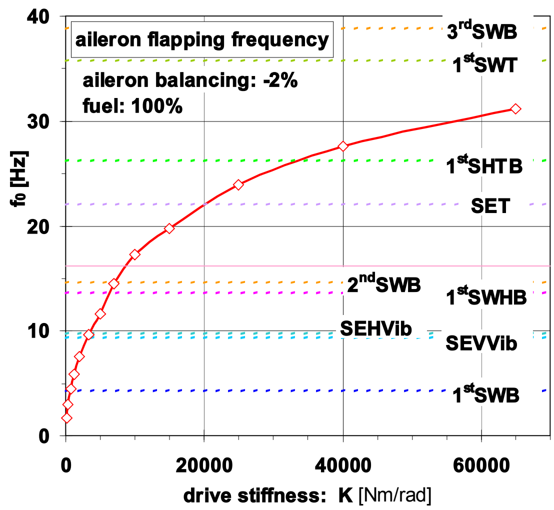

Fig.7: Aileron flapping frequency as a parameter

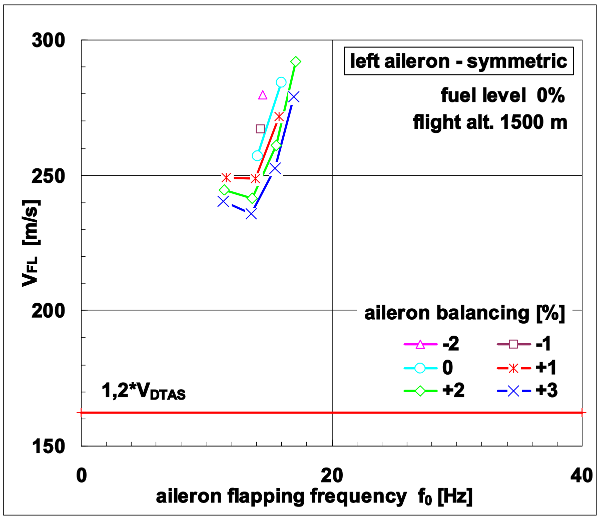

Fig.8: Left aileron flutter – flutter speed (stage 1)

12 configurations with the critical flutter speed, it was the symmetric wing bending – torsion flutter. The $V_{FL} > V_{certif}$ in all the configurations, the level of reserve towards the certification speed was sufficient.

6.2 Controls flutter

Flutter of the control surfaces was investigated separately for the left and right aileron specification, left and right elevator specification and the rudder. Parameters of the other controls remained at the nominal values. As an example, the analyses of the left side aileron flutter will be provided in details. The described evaluation was applied to the other control surfaces as well. In the first stage, there was investigated influence of the following parameters: The wing tank loading (0; 50; 100%); the flight altitude (6 levels); stiffness of the aileron drive (aileron flapping frequency – for example see fig.7); aileron static balancing (+3; +2; +1; 0; -1; -2% - relative balancing with respect to the control mean geometric chord). Obviously, there were investigated both symmetric and antisymmetric boundary conditions, 4536 calculations in total. Parameters for the other control surfaces were chosen in a similar way. Flutter was investigated in the velocity range up to 300 m/s and frequency up to 100 Hz. When the critical state occurred, the secondary calculations were performed to investigate the dominant modes influencing the flutter.

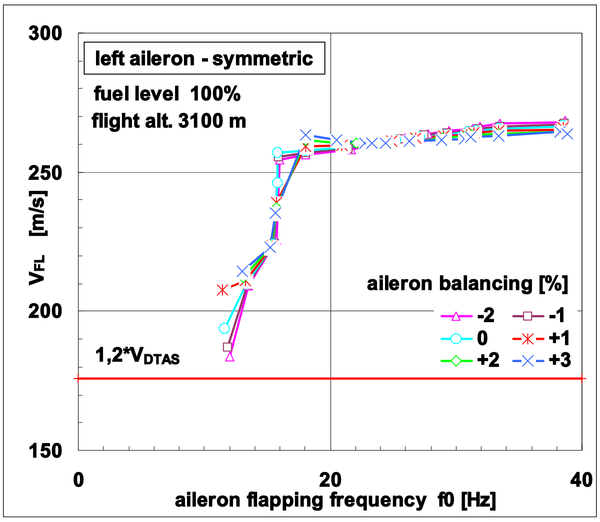

Fig.9: Left aileron flutter – flutter speed (stage 1)

For the symmetric boundary condition, fuel level of 0% and 50%, the critical state occurred, with the flutter frequency around 9.5 Hz and the critical flutter speed about 240.0 m/s. The flutter is characterized by the dominant modes of the wing bending, engine vibration and the wing torsion. More critical are the states of over-balanced aileron (see fig.8). This is a symmetric surface flutter, modified by the aerodynamic and inertia effect of the aileron. The similar type of the flutter was found at the fuel level of 100% as well (see fig.9). The values of the critical flutter speed were lower (minimum reserve towards the certification speed of 5%), than in the former example, so for the next stage of calculations, the fuel

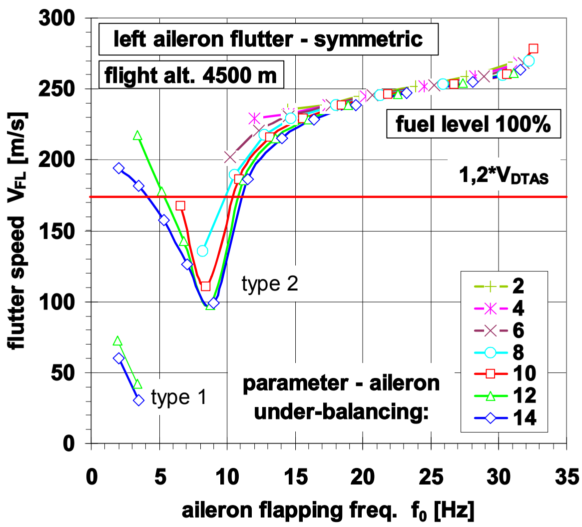

Fig.10: Left aileron flutter – flutter speed (stage 2)

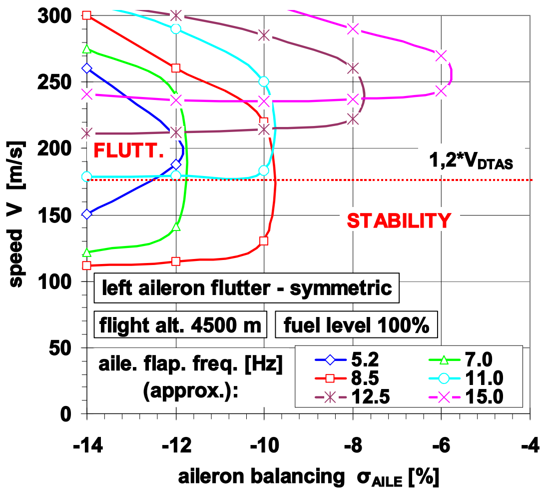

Fig.11: Left aileron flutter – stability boundaries

level of 100% seems to be less favorable.

For the antisymmetric boundary condition, there were found the critical states only for the specific flight altitude and the aileron drive stiffness, critical flutter speed was around 280.0 m/s, flutter frequency around 12.5 Hz, dominant modes are wing bending and torsion. There were found the critical states of the tail flutter as well, however, regarding the space, these results are not presented here.

1st stage calculations represented the practicable ranges of the parameters. In order to describe the flutter occurrence areas and evaluate the reserve towards the certification speed in terms of the balancing level, the ranges of the aileron balancing were extended to large under-balancing <–2%; –14%> and the 2nd stage calculations were performed, 3378 calculations in total. For the symmetric boundary condition, the two types of the flutter were found (see fig.10). For the low aileron flapping frequency and the large under-balancing (>8%), the bending aileron flutter occurs with dominant modes of the wing bending and the engine vertical vibration, flutter frequency is around 4.2 Hz. The second type of the flutter is the aileron bending torsion flutter with the dominant modes of the wing bending, engine vibration and the wing torsion, flutter frequency is around 10.0 Hz. There is a significant drop in the flutter speed around the aileron flapping frequency of 9.0 Hz. Regarding the fuel level, the value of 100% is the most critical. Other kind of the visualization – flutter stability boundaries with respect to the flow speed and the aileron balancing for the type 2 instability is presented in the fig.11. There is also a stability boundaries diagram with the influence of the flight altitude presented in the fig.12. Both critical modes have a typical control flutter hump instability character.

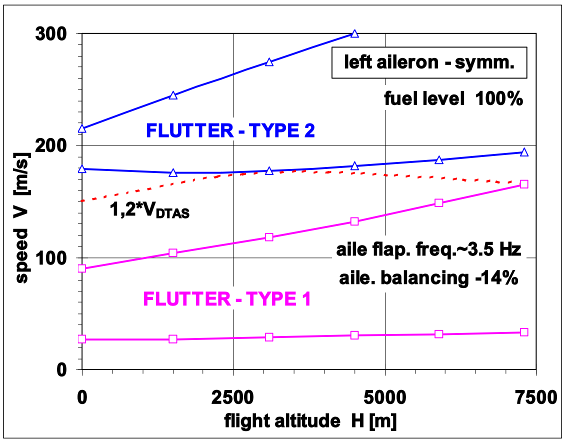

Fig.12: Left aileron flutter – stability boundaries

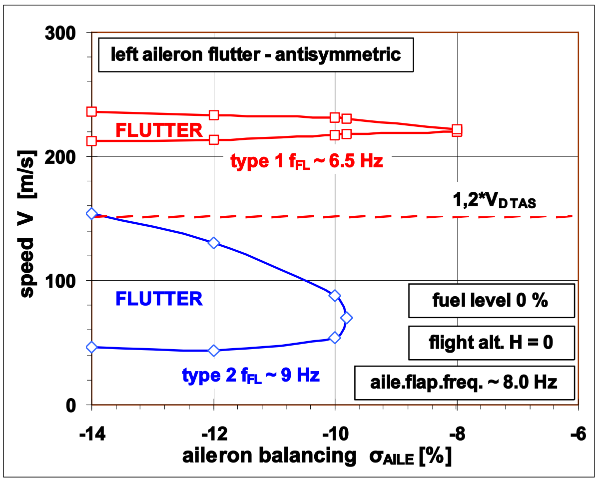

Fig.13: Left aileron flutter – stability boundaries

For the antisymmetric boundary condition, the two types of the instability occurred. The dominant mode shapes are wing – fuselage vibrations and the wing bending (critical frequency around 6.5 Hz, aileron flapping frequency up to 15.0 Hz) and the vertical engine bending (critical frequency around 9.0 Hz, aileron flapping frequency from 5.0 to 10.0 Hz). The example of the flutter boundaries is presented in the fig.13.

6.3 Tab flutter

Flutter of the tabs was investigated for the left aileron tab, right elevator tab and the rudder

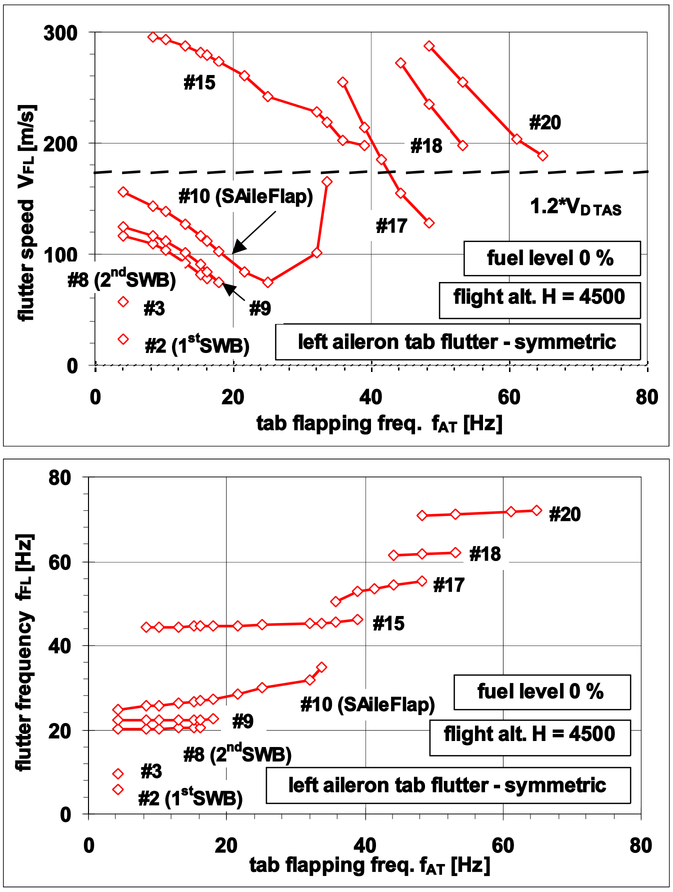

Fig.14: Left aileron tab flutter – flutter speed, frequency

tab. Other controls have no tab. As an example, the analyses of the left aileron tab flutter will be provided in more details. There was investigated influence of the following parameters: The wing tank loading (0; 50; 100%); the flight altitude (6 levels); stiffness of the tab drive - tab flapping frequency (~ 0.0 – 80.0 Hz), both boundary conditions. Since the tab isn't balanced and the hinge is placed at the leading edge, the tab flapping mode induce a flutter due to the large under-balancing with several other modes (see fig.14).

7 GROUND VIBRATRION TEST PREPARATION

GVT test engineers are subjected to two conflicting requirements – to get high quality results in a limited test period. The idea is to shift maximum possible operations to the pre-test period. The exciter locations and determination of forces for a reliable excitation of all investigated modes is the primary factor influencing both the time and the quality. The quality of identified modal parameters strongly depends on the quality of measured data and naturally, quality data can be measured only when investigated mode shapes are appropriately excited.

The preparation procedure is based on utilization of an analytical model and proceeds in following steps: selection of measured points, definition of the reference analytical model, selection of candidate points for excitation and classification of candidate points. Analytical model is defined by modal parameters of 50 modes in the frequency range up to 100 Hz. The grid of 189 selected measured points (see fig. 15) respects calculated mode shapes, symmetry of the aircraft, system of ribs and assumption that stiffness of ribs is enough high so that their deformations in the frequency range up to 100 Hz are negligible small. Analytical mode shapes were transformed to measured points and corresponding generalized masses were recalculated. Modal parameters are completed by common value of the damping ratio. 69 points were selected as candidate points for excitation. Points inaccessible for exciters, on control surfaces and pre-estimated as inappropriate for excitation were excluded. With respect to the symmetry, there are classified 17 single points and 26 paired ones. For

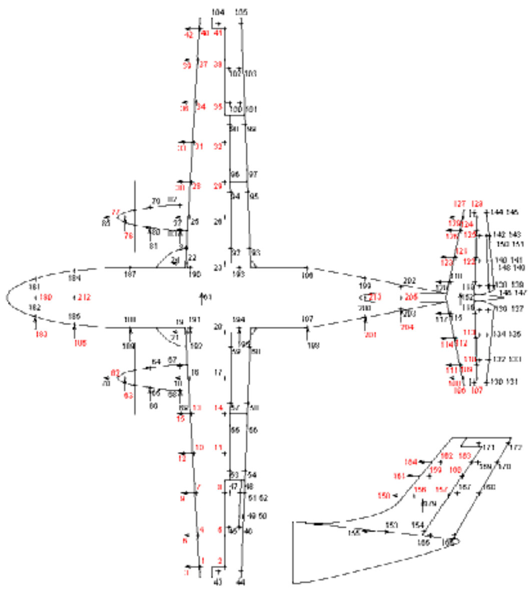

Fig.15: Measured and candidate points for excitation (red)

classification of particular points in terms of their applicability for excitation of a given mode was proposed special classification function ε_j

$$\varepsilon_j = \frac{\sum_{i=1}^{N}\left(\sum_{r=1}^{n}\frac{\phi_{i,r}\phi_{j,r}m_r\left(\omega_r^2-\omega^2\right)}{m_r^{\,2}\left(\omega_r^2-\omega^2\right)^2+4m_r^2\omega_r^2\omega^2\zeta_r^2}\right)^2}{\sum_{i=1}^{N}\left(\sum_{r=1}^{n}\frac{\phi_{i,r}\phi_{j,r}2m_r\omega_r\omega\zeta_r}{m_r^{\,2}\left(\omega_r^2-\omega^2\right)^2+4m_r^2\omega_r^2\omega^2\zeta_r^2}\right)^2} \tag{1}$$

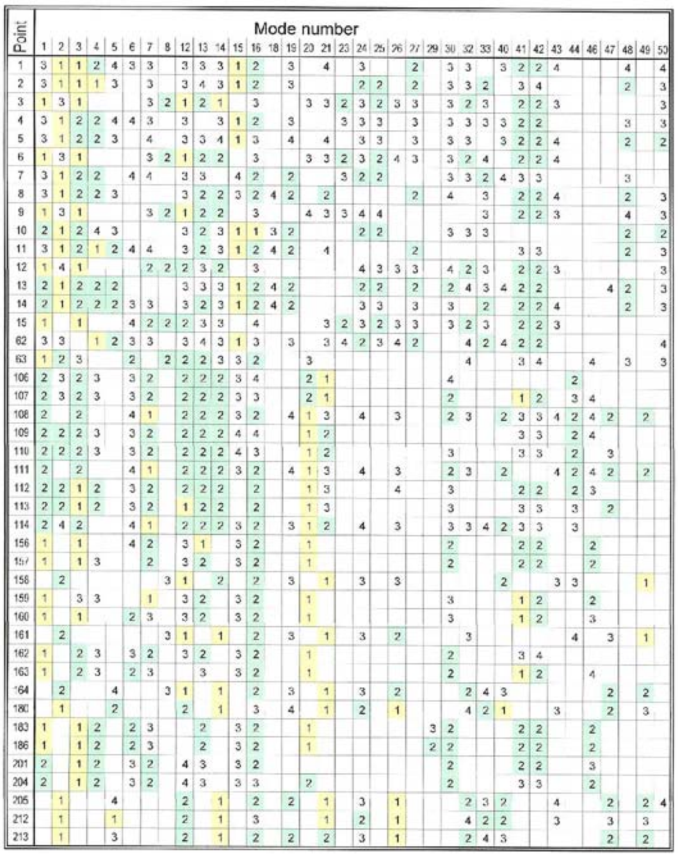

Fig.16: Classification of candidate points for excitation

The function shows the ratio of real and imaginary responses of all N measured points i on the structure excited in one point j in the natural frequency ω_r of analyzed mode r. The function includes influence of all n modes in the frequency range of interest. The function ε_j was calculated for each of candidate points. Points are then classified into groups according to the size of the ε_j. (see fig.16). Calculations of a force needed for excitation is the next classification step. The point from the lowest group that needs the minimal force for excitation will be finally on the first position for excitation of the mode.

The example for a particular mode is presented in the fig.17. Results are sorted so that the first row of the table represents the best point for excitation. The value of the test function represents quality of the excitation. The introduced force is needed for excitation of acceleration 1g of the point with maximal displacement. In the table, there is also information about recommended exciter type and about undesired influence of exciters moving parts on vibration of the tested structure expressed as a change of the natural frequency. Tables are completed with a picture of the mode shape.

No. of excitation point	No. of pairing excitation point	Function ε	Test function group	Excitation force [N]	Exciter type	Influence of exciter [%]
3	42	0.0063	1	34	50	0.07
6	39	0.0064	1	40	200	0.37
9	36	0.0066	1	51	200	0.23
204	0	0.0011	1	65	200	0.28
12	33	0.0068	1	68	200	0.13
201	0	0.0011	1	80	200	0.19
183	0	0.0053	1	95	200	0.13
15	30	0.0072	1	97	200	0.06
186	0	0.0064	1	130	200	0.07
107	128	0.0294	2	15	50	0.31
106	127	0.0280	2	16	50	0.31
110	125	0.0278	2	19	50	0.21
109	124	0.0263	2	19	50	0.21
113	122	0.0249	2	33	50	0.07
108	129	0.0361	2	33	50	0.07
112	121	0.0232	2	34	50	0.07

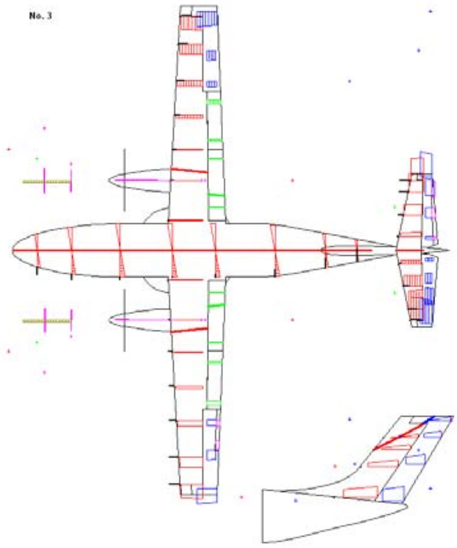

Fig.17: Mode no.3 - recommended excitation points, mode shape visualization

8 WHIRL FLUTTER

The most critical parameters influencing the whirl flutter stability are natural frequencies of the flexibly attached engine – propeller system vibrations (vertical and lateral). The critical parameters are stiffness of the engine system attachment, since the reliable data aren't at disposal until the GVT. On the other side, we can assume the inertia characteristics of the engine – propeller system as reliably determined. Usage of the ordinary analysis approach would lead to the large parametrical studies due to the airworthiness regulations direct requirement to include the changes in the stiffness and damping of the propeller – engine – nacelle – structure system (§23.629(e)(1)(2)). Determination of the parameters, when the whirl flutter speed is equal to the certification speed would considerably decrease number of necessary analyses. Also, the influences of the secondary parameters like wing inertia or stiffness could be easily evaluated.

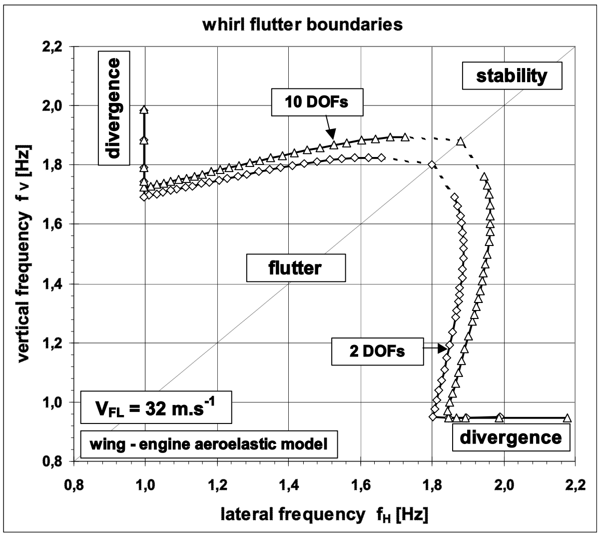

Fig.18: Whirl flutter stability boundaries (critical values of natural frequencies) – approach description

For this purpose, the analytical approach employing the NASTRAN optimization solver (SOL 200) has been prepared. It is based on the three launches of the NASTRAN, the second (main) one is a composite optimization solution for both the normal modes and flutter subcases including the external data, as the ordinary whirl flutter solution. The procedure was tested on a single-engine turboprop model and the twin turboprop scaled aeroelastic component model (see fig.18).

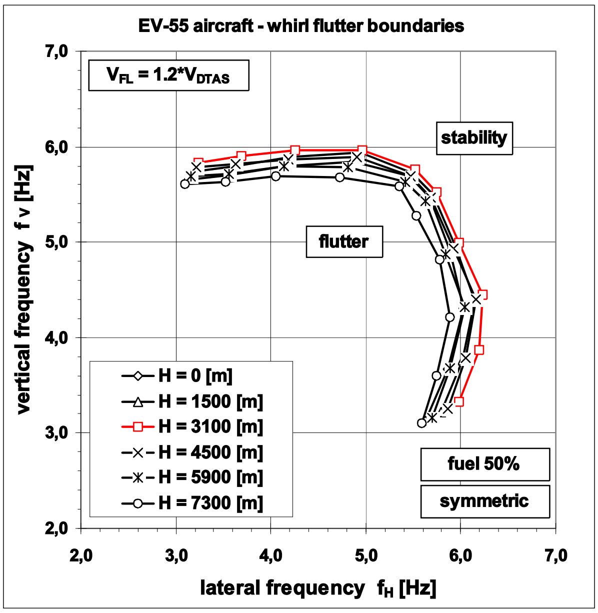

Fig.19: Whirl flutter stability boundaries – parameter: flight altitude

The calculations were performed for both boundary conditions. Analyses included modes in frequency range up to 50.0 Hz. First of all, the influence of the flight altitude was evaluated. As presented in the fig.19, regarding the flight altitude and the relating certification speed, the altitude of 3100 m is the most critical. That's why just this one was used for further analyses. The main parameter was the wing tank loading (0; 25; 50; 75; 100%). There are presented the whirl flutter boundaries for the symmetric boundary condition in the fig.20. For the calculated states, the first three mode shapes were vertical engine bending, horizontal engine bending and 1st wing bending, in any order. The frequency distance between the 1st wing bending and one of the engine vibration modes was the significant factor. Decreasing the 1st wing bending frequency, the frequency distance from critical engine vibration frequencies is increasing. This fact causes the different character of the boundaries for the fuel level of 100%.

9 CONCLUSION AND OUTLOOK

The submitted paper deals with the twin turboprop utility aircraft aeroelasticity. First of all, there is described a plan of certification. The computational model and specific types of analyses are also included. In addition, the preparation of the GVT to find the best points for excitation of in order to reduce the test time and improve quality. Finally, the whirl flutter analyses employing the optimization-based solution to determine critical structure parameters with regard to the stability are described.

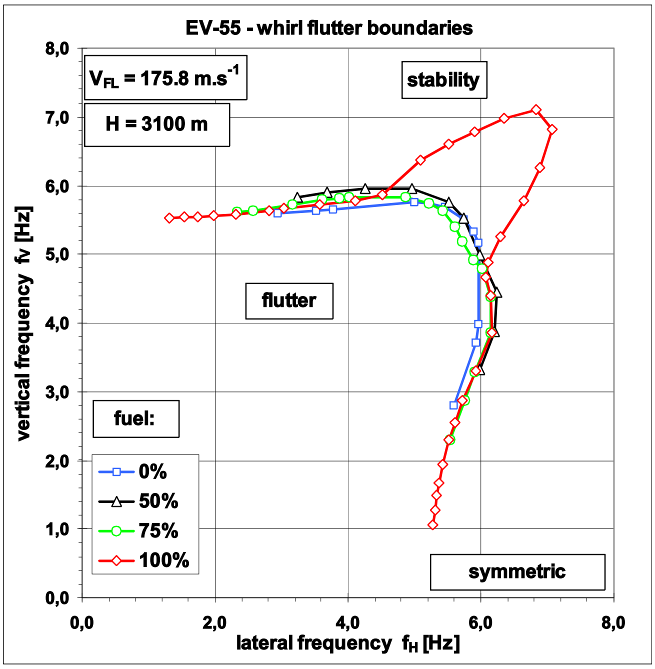

Fig.20: Whirl flutter stability boundaries (critical values of natural frequencies) – EV-55 - symmetric

In the future, the “pre-GVT” calculations will be finished (control flutter, whirl flutter). After the GVT, the computational model will be updated according to the experimental results and the final calculations by means of the experimental data will be performed. Results will be submitted to the certification authority.

10 REFERENCES

[1] FAR Part 23, Amendment 23-52; Advisory Circular No. 23.629-1A

[2] W. P. Rodden and E. H. Johnson, MSC/NASTRAN Aeroelastic Analysis User’s Guide, Version 68, The MacNeal-Schwendler Corp., Los Angeles, CA, 1994.

[3] O.Cerny, V.Hlavaty, “Optimization of Exciter Locations for Modal Testing of Aircraft Structures”, journal Czech Aerospace Proceedings,1/2009, April 2009, pp.17-22, ISSN 1211-877X

[4] J. Cecrdle: “Whirl Flutter Analysis of the Small Transport Aircraft”, IFASD 07 (International Forum on Aeroelasticity and Structural Dynamics, International Conference, 18.6. – 20.6.2007, Stockholm, Sweden, IF-021, CD-ROM

[5] J. Cecrdle: “Exploitation of Optimization Solution for Determination of Whirl Flutter Stability Boundaries”, 26th Congress of the International Council of the Aeronautical Sciences (ICAS 2008), September, 14 – 19, 2008, Anchorage, AK, USA, ICAS2008-P3.2